

PAPER View Article Online
View Journal | View Issue



Cite this: Phys. Chem. Chem. Phys., 2015, 17, 5338

Received 22nd September 2014,

Accepted 5th January 2015
DOI: 10.1039/c4cp04248d

www.rsc.org/pccp

Evidence of "new hot spots" from determining the nonlinear optical behavior of materials: mechanistic studies of the vanadium borate crystal, $Na_3VO_2B_6O_{11}$ †

Xin Su,^{ab} Zhihua Yang,*^a Ming-Hsien Lee,^{ac} Shilie Pan,*^a Ying Wang,^{ab} Xiaoyun Fan,^a Zhenjun Huang^{ab} and Bingbing Zhang^{ab}

A novel mechanism for the nonlinear optical (NLO) effects of vanadium borate crystals, $Na_3VO_2B_6O_{11}$ (NVB), with distorted VO_4 groups was investigated. A comprehensive analysis of the structure-property relationship was performed by combining the experimental measurements, the electronic structures calculations, the SHG-weighted electron density and the real-space atom-contribution analysis to yield the linear and nonlinear optical properties. The contribution of a $(VO_4)^{3-}$ anionic group to the second harmonic generation (SHG) response was more pronounced than that of the $(BO_3)^{3-}$ anionic group, which plays a virtual role in the SHG effects in NVB. The anionic $(BO_3)^{3-}$ groups make dominant contributions to the birefringence, whereas the contribution of the V^{5+} cations to these linear optical effects is negligible.

Introduction

Borate materials, which are crystallographic noncentrosymmetric (NCS), have attracted considerable interest for their potential characteristics, especially in the second-order nonlinear optical (NLO) activity. 1-17 Introducing NCS building units has become an extremely important way of obtaining NCS structures, 18,19-24 such as acentrically distorted units with octahedral coordinated d⁰ transition metals (Nb⁵⁺, V⁵⁺, *etc.*) or lone-pair active cations (Pb²⁺, Bi³⁺) due to the second-order Jahn-Teller (SOJT) effect. 25 Although it has been reported that SOJT distortions are not the only displacement presence in d⁰ materials, 26 an a d⁰ transition metal cation may also distort tetragonally along the *C*4 axis. 27 Introducing a d⁰ transition metal V⁵⁺ into borates can promote the formation of new NCS borate materials. Several vanadium

The existence of vanadium borate, Na₃VO₄B₆O₉, was first obtained in early 2000 by Touboul et al. in the course of their investigation of heating a mixture of Na₂CO₃·H₂O, V₂O₅, and H₃BO₃.²⁸ In 2010, the single crystal of Na₃VO₄B₆O₉ was grown and the crystal structure was described by our group. 30-32 The formula, Na₃VO₄B₆O₉, has been changed to Na₃VO₂B₆O₁₁ (NVB) according to its anionic structure.32 NVB crystallizes in the space group, $P2_12_12_1$, with cell dimensions, a = 7.7359(4) Å, b =18.744(9) Å, c = 12.5697(0) Å, and Z = 4. As shown in Fig. 1, this structure has a three-dimensional framework comprised of B₆O₁₁ units, VO₄ tetrahedra, NaO₇ and NaO₈ polyhedra. The hexa-borate B₆O₁₁ unit consists of three BO₄ units and three BO₃ units are joined together through corner-sharing O atom forming. The VO₄ tetrahedra and sodium atoms are distributed in the channels of the two-dimensional (2D) network of the B-O groups.31

Recent investigations by our group on the linear and non-linear optical (NLO) properties of NVB have highlighted this crystal as a promising material for the SHG effect that gives a similar response to that of KDP, as well as a wide transparency range from 370 to 3000 nm with the shortest SHG wavelength at 427 nm. 32 Considering the origin of the NLO effects in NVB, it is interesting and meaningful to grow a large single crystal and further investigate its structure–property relationship. Since NVB was first reported by Touboul *et al.*, 28 to the best of our knowledge, there have been no theoretical studies on the linear and NLO properties of NVB compound until now, and the mechanism of the SHG response for NVB is still an open question. Thus far, a

borates, such as $Na_3VO_2B_6O_{11}^{28}$ and $K_2SrVB_5O_{12}^{29}$ with non-SOJT-type distortion exhibit interesting NLO properties.

^a Key Laboratory of Functional Materials and Devices for Special Environments of CAS, Xinjiang Key Laboratory of Electronic Information Materials and Devices, Xinjiang Technical Institute of Physics & Chemistry of CAS, 40-1 South Beijing Road, Urumqi 830011, China. E-mail: zhyang@ms.xjb.ac.cn, slpan@ms.xjb.ac.cn

^b University of Chinese Academy of Sciences, Beijing 100049, China

^c Department of Physics, Tamkang University, Taipei 25137, Taiwan

[†] Electronic supplementary information (ESI) available: Experimental details: crystal growth, transmittance spectrum and Refractive-index dispersion measurements. the distortion of the VO₄ tetrahedron in NVB crystal; crystal transmission spectrum and crystal photograph; the experimental SHG phase matching range; selected bond lengths (Å) and angles (deg) for the NVB; State energies (eV) of the highest valence band (H-VB) and the lowest conduction band (L-CB) at same k-points of NVB; the experimental values of refractive indices were measured several wavelengths at room temperature; the nonzero elements of $\chi(2)$ expected for NVB crystal in point group 222. See DOI: 10.1039/c4cp04248d

Paper

Na Na10₈ Na20₈ VO₄

Fig. 1 Ball-and-stick representation of NVB, B_6O_{11} , VO_4 , NaO_7 , and NaO_8 groups in the three-dimensional network. (a) The BO_3 triangle and BO_4 form B_6O_{11} polyhedra. (b) The different coordinations of the NaO_n (n=7, 8) and VO_4 groups, respectively. (c) The black arrows represent the direction of the two-dimensional network of NVB viewed down the a-axis. The Na, V, B, O atoms are drawn as black, green, red, and blue balls, respectively.

tentative viewpoint on the origin of the NLO effect of NVB is that there is structural distortion and d^0 transition metal V^{5+} in the VO₄ asymmetric coordination environments in the crystal. ^{31,32}

In recent years, ab initio energy-band calculations of the linear and nonlinear optical effects for β-BaB₂O₄ (BBO), ³³ LiB₃O₅ (LBO), CsB₃O₅ (CBO), CsLiB₆O₁₀ (CLBO), ³⁴ KBe₂BO₃F (KBBF), ³⁵ $BaAl_2B_2O_7$ (BABO), $K_2Al_2B_2O_7$ (KABO), 36 BiB_3O_6 (BIBO), 37 NaNO2, 38 and KH2PO4 (KDP)39 have been reported along with a satisfactory explanation of the mechanism of NLO effects. In this work, we employed CASTEP, 40 a plane-wave pseudopotential total energy package, to calculate the electronic band structures, and the linear and nonlinear optical properties of the NVB crystal. In addition, combined with the SHG-weighted electron density analysis and the real-space atom-cutting technique, this study analyzed the respective contributions of various transitions among the cations and anionic groups to the optical responses of NVB. In this contribution, we used the above calculation method to analyze the electronic band structures and the mechanism for the linear and nonlinear optical properties of the NVB family and obtain some useful results, which are essential to the design, and search for new NLO crystals. The virtual transition processes between the V cations and neighbor O anions have much larger contributions to the SHG effects compared to the (BO₃)³⁻ anionic groups, even though the latter microscopic units make a dominant contribution to the birefringence in NVB.

Methods and computational details

The first-principles calculations were performed using the plane wave pseudopotential method in the CASTEP package ⁴⁰ based on the density functional theory (DFT). ⁴¹ In the present study, the generalized gradient approximation (GGA) with the Perdew–Burke–Ernzerhof (PBE) functional and the norm-conserving pseudopotential were adopted. ^{42–44} The kinetic energy cut-offs of 750.0 eV and Monkhorst–Pack k-point meshes ⁴⁵ (4 × 3 × 3) with a density of 0.025 Å⁻¹ in the Brillouin zone (BZ) were chosen.

The convergence tests showed that the above computational parameters were sufficiently accurate for the present purposes. Moreover, to account for the effects of localized d orbitals in the transition element, the LDA + U method with the on-site orbital dependent Hubbard $U^{46,47}$ energy term for V was employed for the electronic structure calculations. Different U potentials from 2 to 10 eV for V atoms were adopted for the test calculations. The results showed that the choice of U potential has little influence on the calculated optical properties because it just affects the position of the V 3d orbitals located mainly in the energy region away from the band gap. Although NVB crystals contain a transition metal V, there is no need to use U because the band gap is already reproduced fairly well. This result is similar to a recent study on another material, YAB.

The linear optical properties of NVB are determined by the frequency-dependent dielectric function, $\varepsilon(\omega) = \varepsilon_1(\omega) + i\varepsilon_2(\omega)$, which is connected mainly to the electronic structures. The imaginary part, $\varepsilon_2(\omega)$, of the dielectric function, $\varepsilon(\omega)$, is calculated from the momentum matrix elements between the occupied and unoccupied electronic states and is given by⁴⁹

$$\varepsilon_{2}(\mathbf{q} \to O_{\hat{u}}, h\omega) = \frac{2e^{2}\pi}{\Omega\varepsilon_{0}} \sum_{kcv} \left| \left\langle \varphi_{k}^{c} | u \cdot r | \varphi_{k}^{v} \right\rangle \right|^{2} \delta \left[E_{k}^{c} - E_{k}^{v} - E \right]$$
 (1)

The real part, $\varepsilon_1(\omega)$, can be obtained from the imaginary part, $\varepsilon_2(\omega)$, by the Kramers–Kronig transformation. All other optical constants, such as the absorption spectrum, refractive index and reflectivity, are derived from $\varepsilon_1(\omega)$ and $\varepsilon_2(\omega)$.⁵⁰

Furthermore, to analyse the contribution of the relevant groups to the linear and nonlinear optical properties, and to gain further insight into the structure–property relationship, SHG-weighted electron densities analysis^{51,52} and the real-space atom-cutting method⁵³ were adopted to analyse the origins of the nonlinear optical response of NVB for the first time. The theoretical methods were applied with success in a previous study to analyse the linear refractive indices and SHG coefficients of the NLO crystals.^{54–59}

Results and discussion

A. VO₄ distortion

The geometric parameters of the NVB crystal are given above ³² and the basic structural features are shown in Fig. 1. To further improve the understanding of the structure–property relationships, we analysed the structure of the distorted VO₄ tetrahedra. The distortions of the VO₄ tetrahedra are influenced not only by the electronic structure of cation V⁵⁺ but also by the structure of the bond network, lattice in-commensuration, and cation–cation repulsion, ^{53,60} the probable reasons are as follows: (1) In the lattices, the metal V⁵⁺ ions occupying the Wyckoff 4a positions employ the 4-fold T_d site in the distorted tetrahedra environment of $(VO_4)^{3-}$, with a V–O bond length in the range of 1.6376–1.8557 Å. For comparison, a similar result was obtained for the VO₄ tetrahedron, where the mean value of 1.7265 Å (Table S1, ESI†) corresponds to the mean values found in vanadate, such as $CrVO_4$, ⁶¹ 1.7256 Å; $InVO_4$, ⁶² 1.7263 Å, $In_{0.6}Li_{1.2}VO_4$, ^{63,64} 1.7220 Å

and CuMnVO₄,⁶⁵ 1.7290 Å. (2) The V–O(12), V–O(13) distances of 1.6600 and 1.6610 Å are shorter than those of V–O(1) and V–O(2); 1.8460 and 1.7690 Å, respectively, as shown in Fig. S1 (ESI†). (3) The O(1)–V–O(2) angle of 120° was deviated significantly from 109° for a perfect tetrahedron, which is due to the polar displacement of a d⁰ cation, V⁵⁺. VO₄ with an apparent displacement from the center of the tetrahedron may become the dominant NLO active factor in the SHG response, which can

be proved quantitatively by the results of *ab initio* calculations of the SHG-density and the real-space atom-cutting method.

B. Mulliken atomic population analysis

Mulliken population analysis was performed to gain more insight into the bonding character and to explain the charge transfer in NVB. The calculated results show that the B–O and V–O bonds have more covalent character than the other bonds (Table 1). A greater Mulliken atomic charge assures ionic bonding and a smaller Mulliken atomic charge demonstrates the presence of a covalent bond between the atoms. The atomic charge values of Na, B, O and V are 1.15–1.17, 0.79–0.83, –0.56 to –0.73, and 0.72, respectively. The charge transfer between O and Na is 1.94, which is larger than those between O and B and V, which indicates the ionic character of the bonds between O and Na atoms, and the covalent nature between O and B and V bonds. From the atomic charge, we can determine the percentage ionic character.

The bond distances and calculated Mulliken overlap populations Q are listed in Table 2 to better understand the bonding behavior of NVB. Bond order analysis showed that the Na–O, B–O and V–O bond have values of 0.03–0.07e, 0.56–0.88e and 0.50–0.82e, respectively. In NVB crystal, sodium is characterized by a small overlap population, which further indicates an ionic bond. Therefore, the B–O and V–O bonds show more covalent character than the Na–O bonds.

C. Band structure and density of states

To perform the electronic structure calculations, the experimental crystal structure was adopted initially and then optimized computationally. The resulting unit cell parameters and atomic positions were found to be close to those obtained experimentally. The calculated electronic energy band structure along the high symmetry directions in the BZ is displayed in Fig. 2a. Fig. 2a shows that both the conduction band minimum (CBM) and the valence band

Table 1 Mulliken charge population of Na₃VO₂B₆O₁₁

Atom	Na	В	O	V
Population	1.15-1.17	0.79-0.83	-0.56 to -0.73	0.72

Table 2 Bond distances, d, and Mulliken overlap populations, Q (|e|), for the characteristic atomic pairs in Na₃VO₂B₆O₁₁

Value atomic pair	Bond distances d (Å)	Overlap populations
Na-O	2.6814(6)-2.3930(3)	-0.03-0.07
B-O	1.5277(0)-1.3683(7)	0.56-0.88
V-O	1.8444(5)-1.6604(2)	0.50-0.82

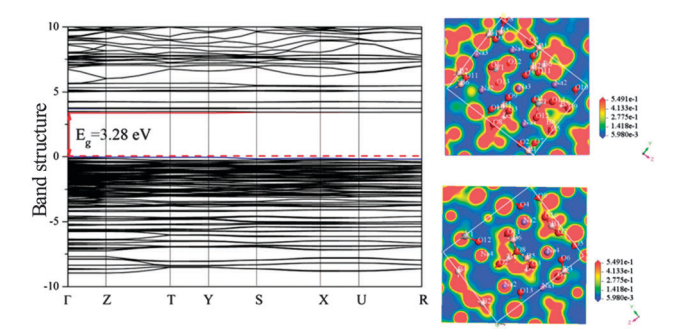


Fig. 2 Electronic band structure along the high-symmetry k-points $(\Gamma - Z - T - Y - S - X - U - R)$ of NVB (left), the highest occupied state was set to 0 eV. The corresponding projected wave function at special energy regions (right): the above and below diagrams are the projected charge density contours of the VO and BO groups, respectively.

maximum (VBM) are located at point Γ , resulting in a direct band gap of 3.28 eV (see Table S2, ESI†), while the corresponding experimental data is 3.35 eV. Moreover, an attempt was made to use other kinds of pseudopotentials to calculate the bands; no apparent change in the results was observed.

As the energy gap is an important issue for the optical property, we paid more attention to obtaining an energy gap closer to the experimental values. To gain a deeper understanding of the band structure features, we plotted slices of the orbital density of the conduction bands (CB) and valence bands (VB) near the band gap, as shown in Fig. 2b. The bands near the band gap were determined from the V–O hybridization states sited at the CB and the states from O and B sited at the VB. In addition, V, B and the neighboring O atoms are characterized by the strong overlap population, which indicates the apparent covalence behaviors agreeing with the data listed in Table 2.

In the present theoretical calculation, the transitions from the occupied states to the unoccupied states were considered. Useful information can be gained from the partial density of states (PDOS), such as the hybridization of states, bonding nature and contribution of orbitals to the electronic band structure. Fig. 3a displays the density of states (DOS) and the partial (PDOS) of the respective species in NVB. The electronic property was obtained by analysing the highest occupied orbitals and lowest unoccupied orbitals in conjunction with the optimized atomic structures. The corresponding calculated optical absorption coefficient spectrum α is shown Fig. 3b. The highest occupied and lowest unoccupied state levels, respectively, come from non-bonding O-2p from the Fermi Level (FL) to about -0.8 eV and the V-O orbits, as shown in Fig. 3c and d. The energy range from -0.8 to -3.0 eV in the VB region has significant contributions from O-2p mixing with the V-3d and B-2p states. In the energy region from -3.0 eV to -9.0 eV, however, the contributions of B-2s and B-2p are apparent in addition to the O-2p states. As for the CBs, the bands above the FL are derived mainly from V-3d, O-2p, B-2p states with a slight contribution of s and p orbitals of Na. Fig. 3 shows that electronic transitions from the VBs to the CBs mainly dominate the intrinsic UV absorption, α , which exhibits many prominent peaks due mainly to the energy subbands. Fig. 3 also shows that the position of the non-bonding oxygen

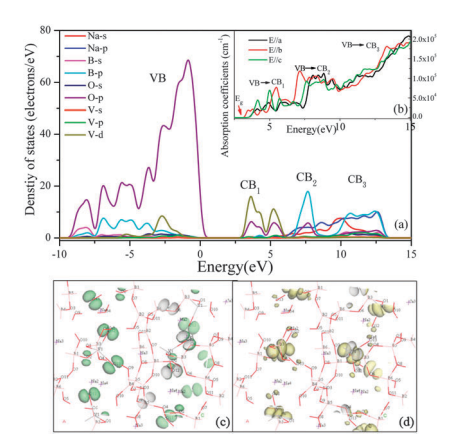


Fig. 3 DOS (a), absorption spectrum (b), the energy range of the specific orbitals of the NVB crystals shown in (c), (d)

and V-O orbits has determines the band gap of the NVB crystals.

D. Optical response

The refractive indices measured by the minimum deviation technique show that NVB is a positive biaxial optical crystal. The calculated refractive indices consist of the experimental ones. The obvious optical anisotropy characterized by n^z-n^x is exhibited in Fig. 4 and Table S3 (ESI†). The calculated and experimental dispersion curves of the refractive indices also display a moderate birefringence around 0.05 at 1064 nm. For practical applications of the NLO crystals as a frequency converter, it should allow the fundamental radiation to remain in phase with those second-harmonic generated, i.e., the phase velocity must be the same for both the second harmonic and the fundamental waves. 66 The phase-matching conditions have been deduced from the calculated refractive indices, as shown in Table S4 (ESI†), which confirms that NVB is phase matchable to the SHG of the 1064 and 532 nm lasers.

The sum-over-states type formalism was proposed to evaluate the SHG coefficients. 67,68 The second-order coefficients, d_{ij} , were

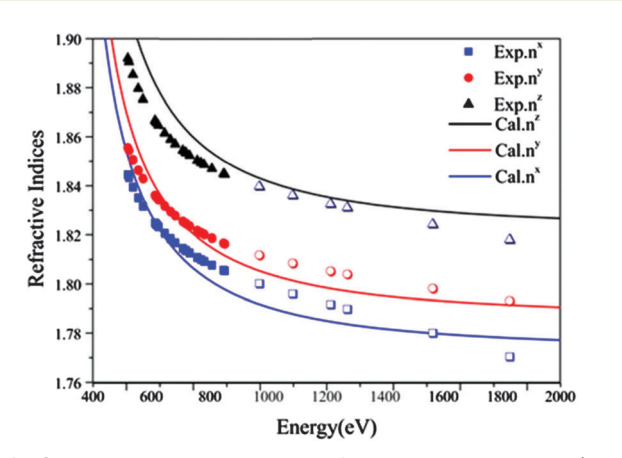


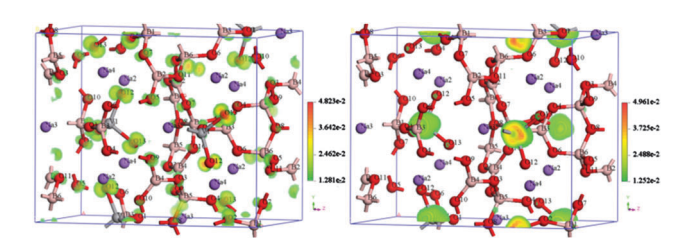
Fig. 4 Calculated and experimental refractive index dispersion (white patterns). The data was fitted using the Sellmeier equations (see in eqn (S2)-(S4), ESI†).

calculated under the static limit within the length gauge. 69,70 There are three nonzero components of the second-order polarizability tensor, namely $d_{14} = d_{25} = d_{36}$, due to the symmetry of NVB. The calculated SHG coefficient, $|d_{14}|$, is 0.45 pm V⁻¹. The $|d_{\text{eff}}^{\text{SHG}}|^{71}$ of NVB crystal for type-I PM in the ZX and YZ planes at the 1064 nm fundamental wavelength are approximately 0.44 pm V⁻¹ and 0.16 pm V^{-1} , respectively (formulae shown in Table S4, ESI†). These coefficients are very close to the experimental powder SHG effect value, which is similar to that of KDP (KH₂PO₄, $|d_{\rm eff}^{\rm SHG}| \approx$ 0.38 pm V⁻¹). Herein, this agreement, as well as other accuracy test results shown in Fig. S3 (ESI†) reconfirmed the validity of this choice of gradient generalized approximation (GGA) approximation in the current study.

E. The SHG-weighted electron densities and real-space atom cutting

We plotted the SHG-weighted electron densities of NVB in Fig. 5. Here we only considered the virtual-electron (VE) because they make dominant contributions to the SHG effects (almost 90% of the total value) in NVB.72-75 Analogous to the alkali metal or alkali earth metal ions in the KBBF-type UV borate NLO crystals, including KBBF,35 KABO, BABO,36 and BABF,52 the Na cations of NVB both in the occupied and unoccupied states have strong ionic characteristics resulting in a spherical symmetric distribution, which shows almost no effect on SHG. The occupied states contributing to SHG come mainly from the B-2p and O-2p orbitals, whereas the unoccupied states are mainly from the V-3d as well as partial B 2p orbitals. This means that the VE processes from the O valence states to the V and B conduction states determine the SHG effects in NVB.

The real-space atom-cutting method was used to investigate the respective contributions of the anionic groups to the birefringence and SHG response of NVB.76 Based on the electron density and SHG-weighted electron density analysis results, 50,77 the microscopic units can naturally be categorized as follows: Na⁺ cations, (BO₃)³⁻, $(BO_4)^{5-}$ groups, and $(VO_4)^{3-}$ groups. The cutting radius of Na was found to be 0.95 Å by investigating the charge-density distribution between the nearest Na and O ions. Following the rule, the cutting radii for the boron, vanadium and oxygen atoms were chosen to be 0.88 Å, 1.2 Å and 1.1 Å, respectively. Table 3 shows that the contribution of the $(VO_4)^{3-}$ group to the refractive indices is comparable to that of the Na⁺ cations, and the $(BO_3)^{3-}$, $(BO_4)^{5-}$ groups. In contrast, the contributions of $(VO_4)^{3-}$ to the birefringence are only about 6.43%, and the contributions of the $(BO_3)^{3-}$ and $(BO_4)^{5-}$ anionic groups are also 46.70%, respectively. In addition, the



Occupied states (left) and unoccupied states (right) in the d_{14} SHG-densities of the NVB crystal in the VE process.

Table 3 Atom-cutting analysis result for the NVB crystal. The sum of the

contributions from the individual groups in the crystal is larger than the original calculated value of the whole crystal due to the repeated calculation of the wave-functions of some shared oxygen atoms

All M ⁺ in unit cell	n^x	n^{y}	n^z	Δn	$d_{14}~(\mathrm{pm}~\mathrm{V}^{-1})$
Origin Na ⁺	1.7888	1.8024	1.8398	0.051	0.4520
	1.1270	1.1281	1.1343	0.0073	-0.0588
$(BO_3)^{3-}$ $(BO_4)^{5-}$ $(VO_4)^{3-}$	1.6728	1.6893	1.6939	0.0211	0.2935
$(BO_4)^{5-}$	1.6709	1.6890	1.6992	0.0283	0.0922
$(VO_4)^{3-}$	1.5334	1.5369	1.5373	0.0039	0.3350
Sum				0.0606	0.6619

Na⁺ cations contribute more than 11.55% to the anisotropy of the refractive indices. The sum of the contributions from the groups is larger than the original calculated value due to the repeated calculation of the wave-functions of some shared oxygen atoms, otherwise they should be almost equal like the situations in KBe₂BO₃F₂, with individual BeO₃F and BO₃ groups. 68 The overlap calculation will not affect the contribution; therefore, for the birefringence of NVB, the relationships of the contribution are $(BO_4)^{5-} - (BO_3)^{3-} > Na^+ - (VO_4)^{3-}$.

Comparatively and interestingly, the contributions from the ions and atomic groups to the SHG response are very different from that to the refractive indices and birefringence. This atom-cutting analysis reveals quantitatively that the main SHG contribution from $(BO_3)^{3-}$ and $(VO_4)^{3-}$ groups is much larger than those from the Na^+ cations and (BO₄)⁵⁻ groups, and the corresponding contributions from the groups, $(VO_4)^{3-}$ and $(BO_3)^{3-}$, to the overall SHG coefficient are about 50.61% and 44.34%, respectively, which are significant larger than other groups in NVB, with the sequence, $(VO_4)^{3-}$ $(BO_3)^{3-} > (BO_4)^{5-} > Na^+$ for the SHG response. Therefore, as indicated in the above-mentioned discussions for the NVB crystal, the $(BO_3)^{3-}$ or $(BO_4)^{5-}$ group is one but not the only one reason for the large NLO effects. The NLO effects originate mainly from the "new hot spots" in the NVB, $(VO_4)^{3-}$ anionic groups.

F. The "new hot spots" as $(VO_4)^{3-}$ groups

According to anionic group theory,76 the nonlinear optical effects mainly come from $(BO_3)^{3-}$ with a small contribution from $(BO_4)^{5-}$ in the borate crystals.^{34,77} In addition, the distorted MO₄ tetrahedron groups, such as $(PO_4)^{3-}$, $(SiO_4)^{4-}$, $(ZnO_4)^{4-}$, and $(AlO_4)^{5-}$ are often employed to design new NLO materials. On the other hand, the $(PO_4)^{3-}$, $(SiO_4)^{4-}$, $(ZnO_4)^{4-}$, and $(AlO_4)^{5-}$ anionic groups make little contribution to the overall microscopic second-order susceptibilities compared to the B-O groups. 78-82 In this paper, using SHG-weighted electron density analysis and the real-space atom-cutting technique, the origin of the nonlinear optical properties of NVB was investigated. As indicated in the above mentioned discussions, the NLO effects of the NVB crystal originate mainly from $(VO_4)^3$ rather than $(BO_3)^{3-}$ and $(BO_4)^{5-}$.

It should be noted that a similar result was obtained in the BIBO³⁷ and YAl₃(BO₃)₄ (YAB), ⁴⁸ in which the contributions from the $(BiO_4)^{5-}$ and $(YO_6)^{9-}$ groups dominate the microscopic second-order susceptibilities. SHG density analysis showed that both Bi and Y cations are not spherical but form significant covalent chemical bonds with the neighbouring O anions, establishing the

(BiO₄)⁵⁻ quadrangular pyramids¹⁵ and deformed (YO₆)⁹⁻ octahedra⁴⁸ as "hot spots"; their contribution to the NLO effect is also much larger than that of the (BO₃)³⁻ groups in BIBO and YAB, respectively.⁵⁹ Therefore, the real-space atom-cutting technique shows that the NLO effect in these crystals does not originate mainly from the B-O anionic groups, and the contribution from the Bi-O or Y-O groups is even more important. The fact that the contribution of the distorted $(VO_4)^{3-}$ groups is larger than that of $(BO_3)^{3-}$ provide "new hot spots" in that in addition to the $(BiO_4)^{5-}$ quadrangular pyramids and deformed $(YO_6)^{9-}$ octahedra, distorted $(VO_4)^{3-}$ groups can also be used to design new NLO compounds with enhanced SHG coefficients.

Conclusions

On a theoretical front, this comprehensive ab initio study of the linear and nonlinear optical properties of NVB agrees very well with the experimental observations. The top of the valence bands are dominated by the O 2p orbitals, while the bottom of the conduction bands are composed mainly of V 3d and B 2p orbitals. Based on the electronic structure, the refractive indices and SHG coefficients were calculated, which are in good agreement with the experimental values. The combined SHG-weighted electron density analysis with the real-space atom-cutting method showed that the (BO₃)³⁻ anionic groups have a dominant contribution to the linear optical properties, while the $(VO_4)^{3-}$ tetrahedra play a virtual role to the SHG effects in NVB. The theoretical results not only demonstrate that NVB is a potential SHG material for blue wavelength applications, but also identified "new hot spots", (VO₄)³⁻, in addition to the well-known (BO₃)³⁻ that was proven to produce large microscopic second-order susceptibilities in this crystal, which is an important indication for future material design.

Acknowledgements

This study was supported by the National Key Basic Research Program of China (Grant No. 2014CB648400, 2012CB626803), the "Western Light Joint Scholar Foundation" Program of CAS (Grant No. LHXZ201101), the "National Natural Science Foundation of China" (Grant No. 11474353, 11104344), the Recruitment Program of Global Experts (1000 Talent Plan, Xinjiang Special Program), Major Program of Xinjiang Uygur Autonomous Region of China during the 12th Five-Year Plan Period (Grant No. 201130111); NCHC for database resources support, and Key Win Electronics Co. for equipment donation and Xinjiang Program of Introducing High-Level Talents are highly appreciated by MHL.

Notes and references

1 B. H. T. Chai, Optical Crystals, in CRC Handbook of Laser Science and Technology Supplement 2: Optical Materials, ed. M. J. Weber, CRC Press, Boca Raton, FL, 1995, pp. 3-65; C. T. Chen, T. Sasaki, R. K. Li, Y. C. Wu, Z. S. Lin, Y. Mori, Z. Hu, J. Wang, S. Uda, M. Yoshimura and Y. Kaneda,

- Nonlinear Optical Borate Crystals, Weily-VCH Germany, 2012, pp. 1–9.
- 2 K. M. Ok and P. S. Halasyamani, *Chem. Mater.*, 2006, 18, 3176–3183; K. M. Ok, E. O. Chi and P. S. Halasyamani, *Chem. Soc. Rev.*, 2006, 35, 710–717.
- 3 A. H. Reshak, S. Auluck, I. V. Kityk, A. Majchrowski, D. Kasprowicz, M. Drozdowski, J. Kisielewski, T. Lukasiewicz and E. Michalski, *J. Mater. Sci.*, 2006, **41**, 1927–1932.
- 4 A. H. Reshak, S. Auluck and I. V. Kityk, *Phys. Rev. B: Condens. Matter Mater. Phys.*, 2007, 75, 245120.
- 5 A. H. Reshak, X. A. Chen, S. Auluck and I. V. Kityk, J. Chem. Phys., 2008, 129, 204111.
- 6 A. H. Reshak, S. Auluck, A. Majchrowski and I. V. Kityk, Solid State Sci., 2008, 10, 1445–1448.
- 7 A. H. Reshak, S. Auluck and I. V. Kityk, *Appl. Phys. A: Mater. Sci. Process.*, 2008, 91, 451–457.
- 8 A. H. Reshak, X. A. Chen, I. V. Kityk and S. Auluck, *Curr. Opin. Solid State Mater. Sci.*, 2007, **11**, 33–39.
- 9 A. H. Reshak, S. Auluck and I. V. Kityk, J. Alloys Compd., 2008, 460, 99–102.
- 10 A. H. Reshak, S. Auluck and I. V. Kityk, J. Phys.: Condens. Matter, 2008, 20, 145209.
- 11 A. H. Reshak, S. Auluck and I. V. Kityk, *J. Solid State Chem.*, 2008, **181**, 789–795.
- 12 A. H. Reshak, X. A. Chen, S. Auluck, I. V. Kityk, K. Iliopoulos, S. Couris and R. Khenatah, *Curr. Opin. Solid State Mater.* Sci., 2009, 12, 26–31.
- 13 A. H. Reshak, S. Auluck, A. Majchrowski and I. V. Kityk, *Jpn. J. Appl. Phys.*, 2009, 48, 011601.
- 14 A. H. Reshak, S. Auluck and I. V. Kityk, J. Phys. D: Appl. Phys., 2009, 42, 085406.
- 15 A. H. Reshak, X. A. Chen, F. P. Song, S. Auluck and I. V. Kityk, *J. Phys.: Condens. Matter*, 2009, **21**, 205402.
- 16 A. H. Reshak, S. Auluck and I. V. Kityk, *J. Phys. Chem. A*, 2009, **113**(8), 1614–1622.
- 17 A. H. Reshak, S. Auluck and I. V. Kityk, *J. Phys. Chem. B*, 2009, **113**(34), 11583.
- 18 A. H. Reshak, V. V. Atuchin, S. Auluck and I. V. Kityk, J. Phys.: Condens. Matter, 2008, 20, 325234.
- 19 A. H. Reshak, S. Auluck, I. V. Kityk, A. Perona and B. Claudet, *J. Phys.: Condens. Matter*, 2008, **20**, 325213.
- 20 A. H. Reshak and S. Auluck, *Solid State Commun.*, 2008, **145**, 571–576.
- 21 A. H. Reshak and D. Ortíz Andrés Ordóñez, *J. Phys. Chem. B*, 2009, **113**, 13208–13215.
- 22 A. H. Reshak, R. Khenata, I. V. Kityk, K. J. Plucinski and S. Auluck, J. Phys. Chem. B, 2009, 113(17), 5803–5808.
- 23 A. H. Reshak, S. Auluck and I. V. Kityk, *Curr. Opin. Solid State Mater. Sci.*, 2009, **12**, 14–18.
- 24 H. P. Wu, S. L. Pan, K. R. Poeppelmeier, H. Y. Li, D. Z. Jia, Z. H. Chen, X. Y. Fan, Y. Yang, J. M. Rondinelli and H. Luo, J. Am. Chem. Soc., 2011, 133, 7786–7790; H. P. Wu, H. W. Yu, Z. H. Yang, X. L. Hou, X. Su, S. L. Pan, K. R. Poeppelmeier and J. M. Rondinelli, J. Am. Chem. Soc., 2013, 135, 4215–4218; H. P. Wu, H. W. Yu, S. L. Pan, Z. J. Huang, Z. H. Yang, X. Su and K. R. Poeppelmeier, Angew. Chem., Int.

- Ed., 2013, **52**, 3406–3410; F. Li, S. L. Pan, X. L. Hou and Z. X. Zhou, *J. Cryst. Growth*, 2010, **312**, 2383; F. Li and S. L. Pan, *J. Cryst. Growth*, 2011, **318**, 629.
- H. S. Ra, K. M. Ok and P. S. Halasyamani, J. Am. Chem. Soc., 2003,
 125, 7764–7765; C. F. Sun, C. L. Hu, X. Xu, B.-P. Yang and J. G. Mao, J. Am. Chem. Soc., 2011, 133, 5561–5572; J. Zhang, Z. Zhang, W. Zhang, Q. Zheng, Y. Sun, C. Q. Zhang and X. T. Tao, Chem. Mater., 2011, 33, 3752–3761; Y. Z. Huang, L. M. Wu, X. T. Wu, L. H. Li, L. Chen and Y. F. Zhang, J. Am. Chem. Soc., 2010, 132, 12788; W. L. Zhang, W. D. Cheng, H. Zhang, L. Geng, C. S. Lin and Z. Z. He, J. Am. Chem. Soc., 2010, 132, 1508–1509.
- 26 M. Kunz and I. D. Brown, J. Solid State Chem., 1995, 115, 395–406.
- 27 J. B. Goodenough and J. M. Longo, Crystallographic and magnetic properties of perovskite and perovskite-related compounds, in *Landolt-Bornstein*, ed. K. Hellwege, Springer-Verlag, Berlin, 1970, vol. 4, pp. 126–314.
- 28 M. Touboul, N. Penin and G. Nowogrocki, J. Solid State Chem., 2000, 150, 342–346.
- 29 S. J. Chen, S. L. Pan, W. W. Zhao and H. W. Yu, *Dalton Trans.*, 2012, 41, 9202–9208.
- 30 X. Y. Fan, S. L. Pan, J. Han, X. L. Tian and Z. X. Zhou, J. Synth. Cryst., 2010, 39, 35–42.
- 31 X. Y. Fan, S. L. Pan, X. L. Hou, X. L. Tian and J. Han, *J. Cryst. Growth*, 2010, **312**, 2263–2266.
- 32 X. Y. Fan, S. L. Pan, X. L. Hou, X. L. Tian and J. Han, *Cryst. Growth Des.*, 2010, **10**, 252–256.
- 33 C. T. Chen, B. C. Wu, A. Jiang and G. You, *Sci. Sin., Ser. B* (*Engl. Ed.*), 1985, **28**, 235.
- 34 Z. S. Lin, J. Lin, Z. Z. Wang, C. T. Chen and M. H. Lee, *Phys. Rev. B: Condens. Matter Mater. Phys.*, 2000, **62**, 1757.
- 35 Z. S. Lin, Z. Z. Wang, C. T. Chen, S. K. Chen and M. H. Lee, *Chem. Phys. Lett.*, 2003, **367**, 523–527.
- 36 Z. S. Lin, Z. Z. Wang, C. T. Chen, S. K. Chen and M. H. Lee, J. Appl. Phys., 2003, 93, 9717–9723.
- 37 Z. S. Lin, Z. Z. Wang, C. T. Chen and M. H. Lee, *J. Appl. Phys.*, 2001, **90**, 5585.
- 38 Z. S. Lin, Z. Z. Wang, C. T. Chen and M. H. Lee, *Acta Phys. Sin.*, 2003, **50**, 1145–1149.
- 39 Z. S. Lin, Z. Z. Wang, C. T. Chen and M. H. Lee, *Chem. Phys.*, 2003, **118**, 2349–2356.
- 40 S. J. Clark, M. D. Segall, C. J. Pickard, P. J. Hasnip, M. J. Probert, K. Refson and M. C. Payne, *Z. Kristallogr.*, 2005, 220, 567–570.
- 41 B. G. Pfrommer, M. Cote, S. G. Louie and M. L. Cohen, *J. Comput. Phys.*, 1997, 131, 233–240.
- 42 J. P. Perdew, K. Burke and M. Ernzerhof, *Phys. Rev. Lett.*, 1996, 77, 3865–3868.
- 43 J. S. Lin, A. Qteish, M. C. Payne and V. Heine, *Phys. Rev. B: Condens. Matter Mater. Phys.*, 1993, 47, 4174–4180.
- 44 A. M. Rappe, K. M. Rabe, E. Kaxiras and J. D. Joannopoulos, *Phys. Rev. B: Condens. Matter Mater. Phys.*, 1990, 41, 1227–1230.
- 45 H. J. Monkhorst and J. D. Pack, *Phys. Rev. B: Solid State*, 1976, **13**, 5188–5192.
- 46 M. Cococcioni and S. de Gironcoli, *Phys. Rev. B: Condens. Matter Mater. Phys.*, 2005, **71**, 035105.

- 47 S. L. Dudarev, G. A. Botton, S. Y. Savrasov, C. J. Humphreys and A. P. Sutton, *Phys. Rev. B: Condens. Matter Mater. Phys.*, 1998, 57, 1505–1509.
- 48 R. He, Z. S. Lin, M. H. Lee and C. T. Chen, *J. Appl. Phys.*, 2011, **109**, 103510.
- 49 E. D. Palik, *Handbook of Optical Constants of Solids. Orlando*, Academic Press, New York, 1985.
- 50 F. Wooten, Optical Properties of Solid, Academic, New York, 1972.
- 51 M. H. Lee, C. H. Yang and J. H. Jan, *Phys. Rev. B: Condens. Matter Mater. Phys.*, 2004, **70**, 235110.
- 52 H. Huang, Z. S. Lin, L. Bai, Z. G. Hu and C. T. Chen, J. Appl. Phys., 2009, 106, 103107.
- 53 M. Kunz and I. D. Brown, *J. Solid State Chem.*, 1995, **115**, 395–406.
- 54 X. Su, Y. Wang, Z. H. Yang, X. C. Huang, S. L. Pan, F. Li and M. H. Lee, J. Phys. Chem. C, 2013, 117, 14149–14157.
- 55 B. B. Zhang, Z. H. Yang, Y. Yang, M. H. Lee, S. L. Pan, Q. Jing and X. Su, *J. Mater. Chem. C*, 2014, 2, 4133–4141.
- 56 Q. Jing, X. Y. Dong, Z. H. Yang, S. L. Pan, B. B. Zhang, X. C. Huang and M. W. Chen, J. Solid State Chem., 2014, 219, 138–142
- 57 Z. S. Lin, J. Lin, Z. Z. Wang, Y. C. Wu, N. Ye, C. T. Chen and R. K. Li, J. Phys.: Condens. Matter, 2001, 13, 369–384.
- 58 D. S. Wang, Bull. Mater. Sci., 2003, 26, 159-163.
- 59 Z. S. Lin, X. X. Jiang, L. Kang, P. F. Gong, S. Y. Luo and M. H. Lee, J. Phys. D: Appl. Phys., 2014, 47, 253001.
- 60 P. S. Halasyamani, *Chem. Mater.*, 2004, **16**, 3586–3592. And references cited therein.
- 61 M. Touboul, S. Denis and L. Seguin, *Eur. J. Solid State Inorg. Chem.*, 1995, 32, 577–588.
- 62 M. Touboul, K. Melghit, P. Bénard and D. Loüer, *J. Solid State Chem.*, 1995, **118**, 93-98.
- 63 M. Touboul and P. Tolédano, Acta Crystallogr., Sect. B: Struct. Crystallogr. Cryst. Chem., 1980, 36, 240-255.
- 64 M. Touboul and P. Tolédano, *J. Solid State Chem.*, 1981, 38, 386–393.
- 65 H. B. Yahia, E. Gaudin and J. Darriet, *Inorg. Chem.*, 2005, 44, 3087–3093.

- 66 S. N. Rashkeev, W. R. L. Lambrecht and B. Segall, *Phys. Rev. B: Condens. Matter Mater. Phys.*, 1998, 57, 3905–3919.
- 67 S. N. Rashkeev and W. R. L. Lambrecht, *Phys. Rev. B: Condens. Matter Mater. Phys.*, 2001, **63**, 165212.
- 68 C. W. Chen, M. H. Lee and Y. T. Lin, Appl. Phys. Lett., 2006, 89, 223105.
- 69 V. G. Dmitriev, G. G. Gurzadyan and D. N. Nikogosyan, *Handbook of Nonlinear Optical Crystals*, Springer-Verlag Berlin Heidelberg, 2008, pp. 22–29; C. Aversa and J. E. Sipe, *Phys. Rev. B: Condens. Matter Mater. Phys.*, 1995, 52, 14636–14645.
- 70 C. T. Chen, Y. C. Wu, A. D. Jiang, G. M. You, R. K. Li and S. J. Lin, J. Opt. Soc. Am. B, 1989, 6, 616–621.
- 71 B. C. Wu, D. Y. Tang, N. Ye and C. T. Chen, *Opt. Mater.*, 1996, 5, 105–109.
- 72 J. Goodey, J. Broussard and P. S. Halasyamani, *Chem. Mater.*, 2002, **14**, 3174.
- 73 S. N. Rashkeev and W. R. Lambrecht, *Phys. Rev. B: Condens. Matter Mater. Phys.*, 2001, **63**, 165212.
- 74 J. Lin, M. H. Lee, Z. P. Liu, C. T. Chen and C. J. Pickard, *Phys. Rev. B: Condens. Matter Mater. Phys.*, 1999, **60**, 13380–13389.
- 75 C. H. Lo and M. H. Lee, *The Role of Electron Lone-pair in the Optical Nonlinearity of Oxide, Nitride and Halide Crystals*, Master thesis, Taiwan, 2005, p. 29.
- 76 C. T. Chen, N. Ye, J. Lin, J. Jiang, W. R. Zeng and B. C. Wu, Adv. Mater., 1999, 11, 1071–1078.
- 77 C. T. Chen, in *Development of New Nonlinear Optical Crystals in the Borate Series*, ed. V. S. Letokhov, C. V. Shank, Y. R. Shen and H. Walther, Harwood Academic, Chur, 1993.
- 78 E. P. Zhang, S. G. Zhao, J. X. Zhang, J. P. Fu and J. Y. Yao, *Acta Crystallogr., Sect. E: Struct. Rep. Online*, 2011, **67**, i3.
- 79 B. H. Lei, Q. Jing, Z. H. Yang, B. B. Zhang and S. L. Pan, J. Mater. Chem. C, 2014, DOI: 10.1039/C4TC02443E.
- 80 H. P. Wu, H. W. Yu, S. L. Pan, Z. J. Huang, Z. H. Yang, X. Su and K. R. Poeppelmeier, *Angew. Chem., Int. Ed.*, 2013, 52, 3406–3410.
- 81 Z. S. Lin, Z. Z. Wang, C. T. Chen, S. K. Y. Chen and M. H. Lee, *J. Appl. Phys.*, 2003, **93**, 9717–9723.
- 82 H. Huang, Z. S. Lin, L. Bai, Z. G. Hu and C. T. Chen, *J. Appl. Phys.*, 2009, **106**, 103107.